

Supporting Information

Radially-controlled ZnS interlayer on ultra-long ZnO–Gd₂S₃ core–shell nanorod arrays for promoting the visible photocatalytic degradation of antibiotics

Kugalur Shanmugam Ranjith^a, D. Ranjith Kumar^b, Seyed Majid Ghoreishian^c, Yun Suk Huh^{*,c}
Young Kyu Han^{*,a}, R. T. Rajendra Kumar^{*,b}

^a*Department of Energy and Material Engineering, Dongguk University, Seoul 04620, Republic of Korea.*

^b*Advanced Materials and Devices Laboratory (AMDL), Department of Nanoscience and Technology, Bharathiar University, Coimbatore-641 046, India.*

^c*Department of Biological Engineering, Inha University, Incheon 22122, Republic of Korea*

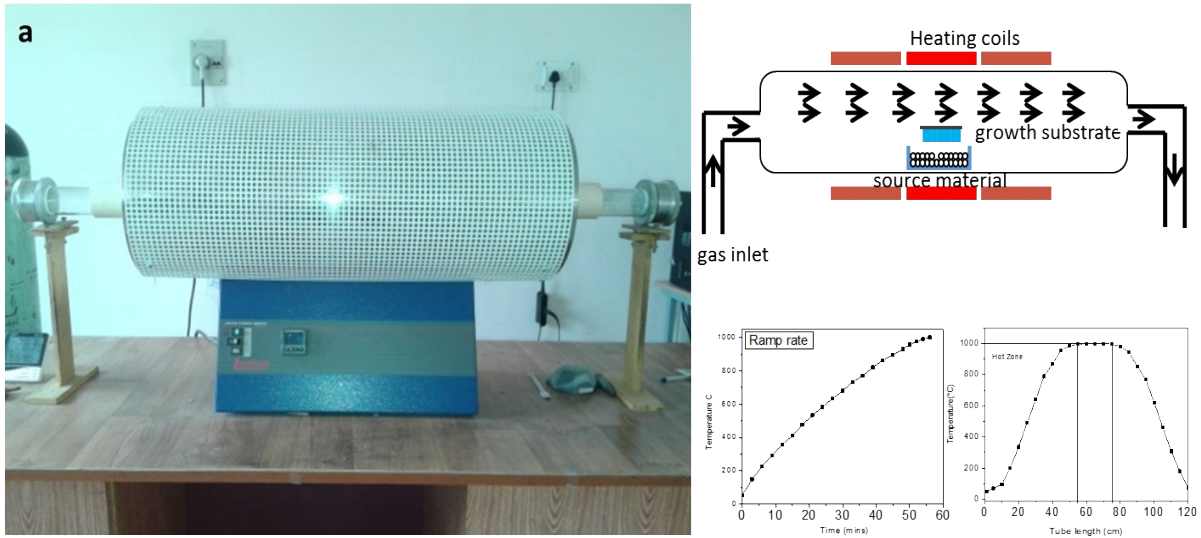


Fig. S1 (a) Photograph and Schematic representation of the growth setup and (b) temperature ramp profile of the tubular furnace.

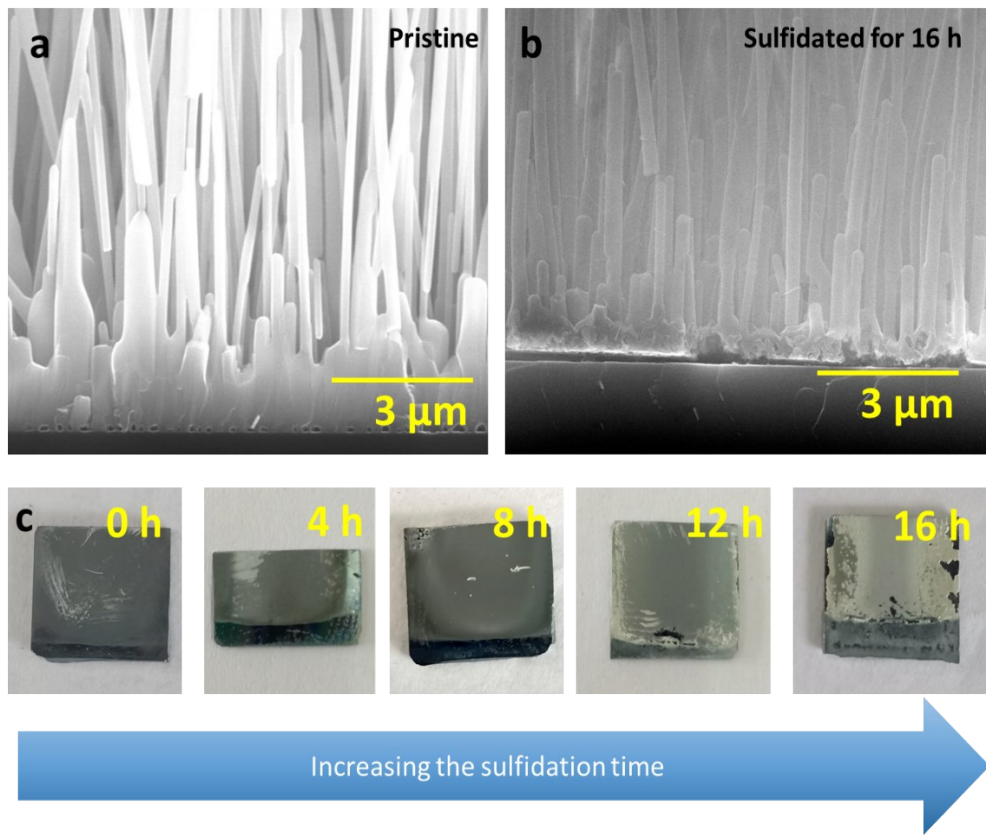


Fig. S2 (a-b) ZnO NR arrays stability before and after the sulfidation time of 16 h, (c) optical images of ZnO-ZnS-Gd₂S₃ NR grown Si substrate with respective to sulfidation time.

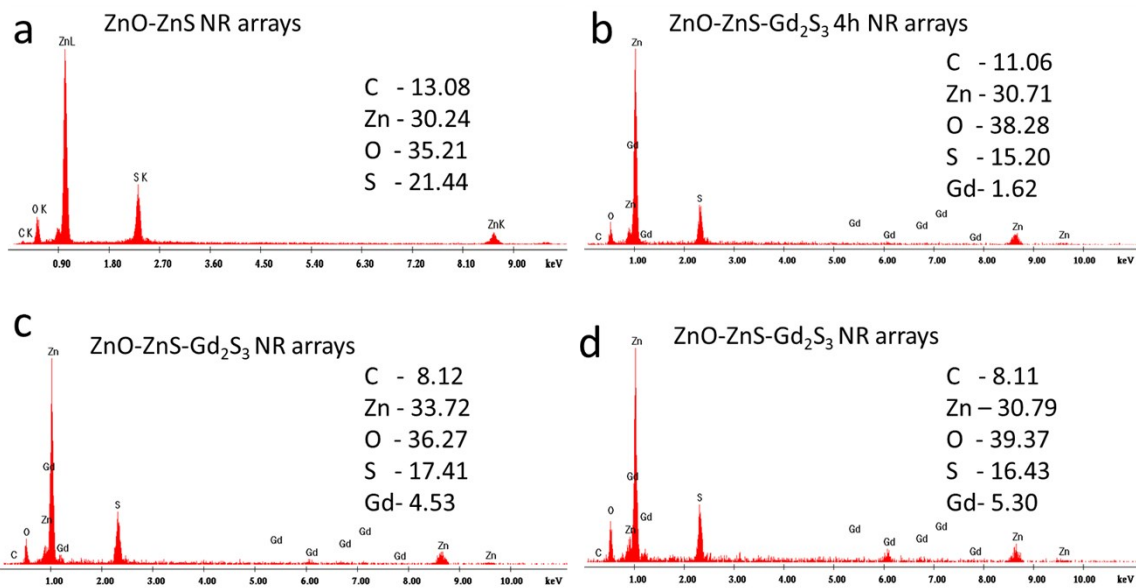


Fig. S3 EDAX spectra of the vertically aligned sulfidated ZnO-ZnS-Gd₂S₃ NR arrays under different reaction time (a) ZnO-ZnS in 8h, (b) ZnO-ZnS-Gd₂S₃ in 4h, (c) ZnO-ZnS-Gd₂S₃ in 8h and (d) ZnO-ZnS-Gd₂S₃ in 12h.

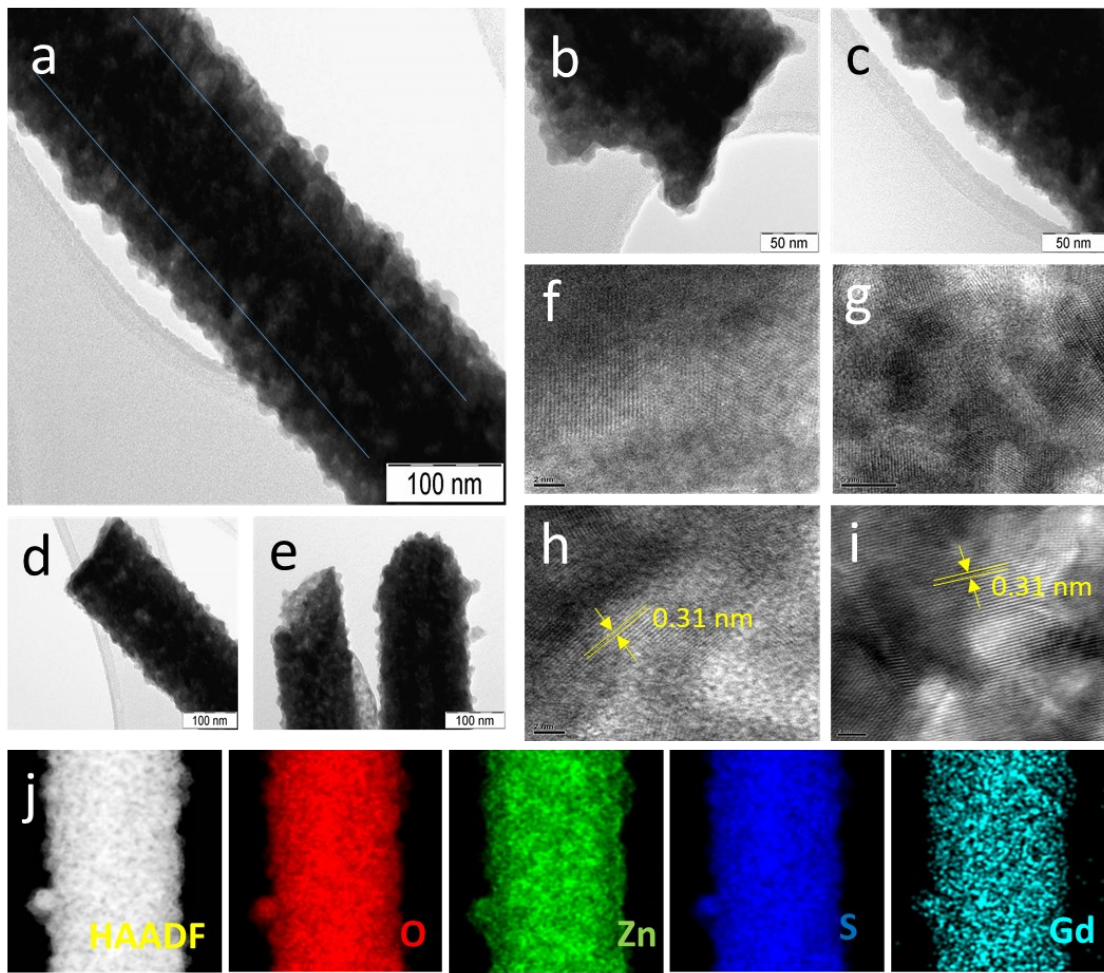


Fig. S4 (a-e) TEM, (f-i) HETEM and (j) elemental mapping results of images of the ZnO-ZnS-Gd₂S₃ (12h) core-shell NR arrays.

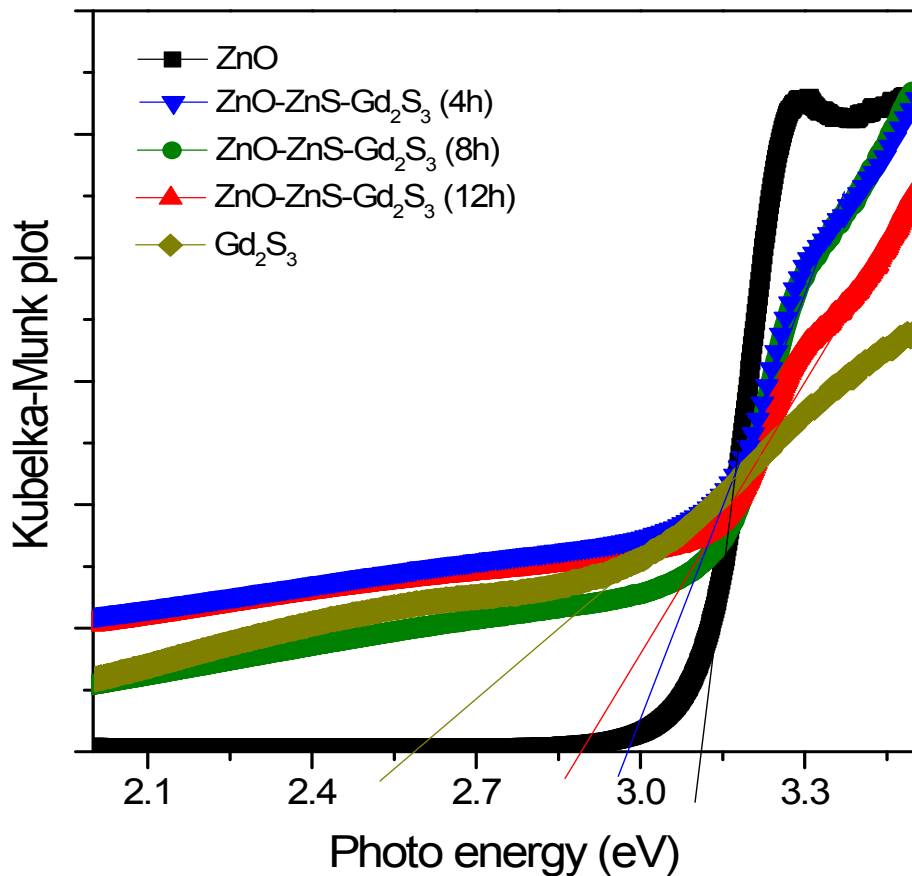


Fig. S5 K-M plot of the different hour sulfidated ZnO-ZnS-Gd₂S₃ hybrid NR arrays.

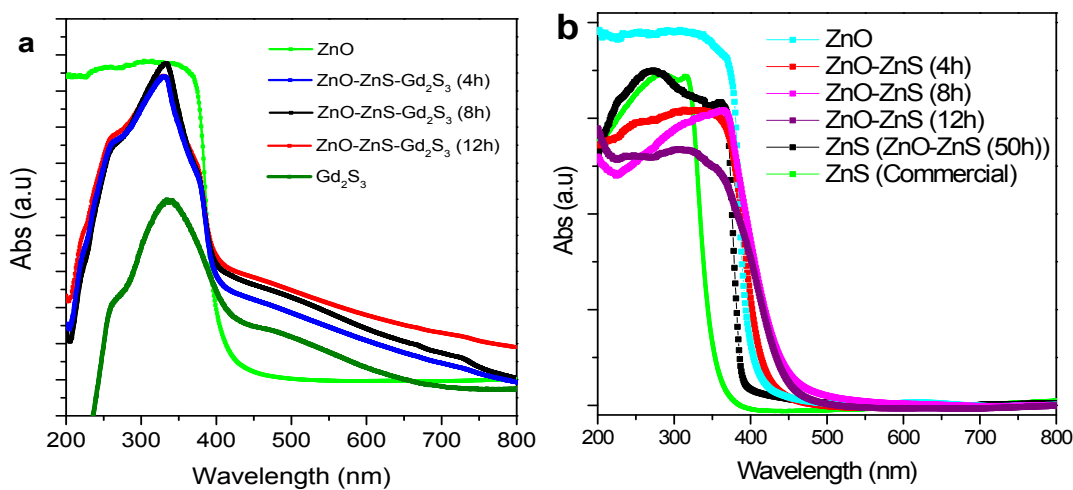


Fig. S6 UV DRS spectra of the (a) shell wall controlled ZnO-ZnS-Gd₂S₃ and (b) ZnO-ZnS core-shell NR arrays.

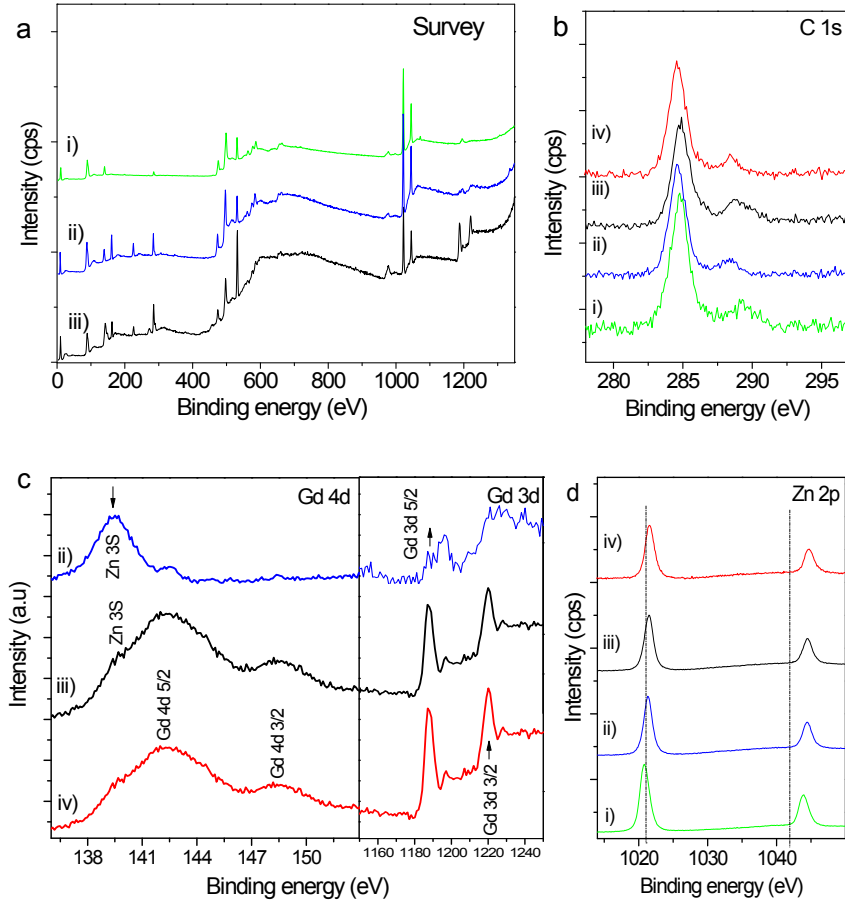


Fig. S7 XPS survey spectra of sulfidated ZnO–ZnS–Gd₂S₃ core–shell NR arrays. (a), high-resolution XPS spectra of the C1s region (b), Gd 4d and 3d region (c), Zn 2p region (d) of pristine (i), 4h (ii), 8h (iii) and 12h (iv) sulfidated ZnO–ZnS–Gd₂S₃ core–shell NR arrays.

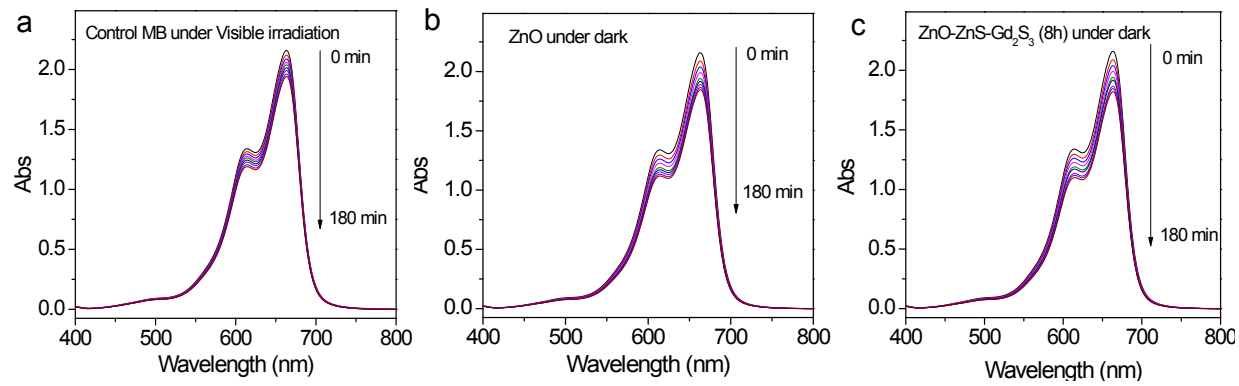


Fig. S8 Photocatalytic activity in absence of (a) catalyst under visible irradiation and activity in dark with the presence of (b) ZnO NR arrays and (c) ZnO-ZnS-Gd₂S₃ (8h) catalyst respectively.

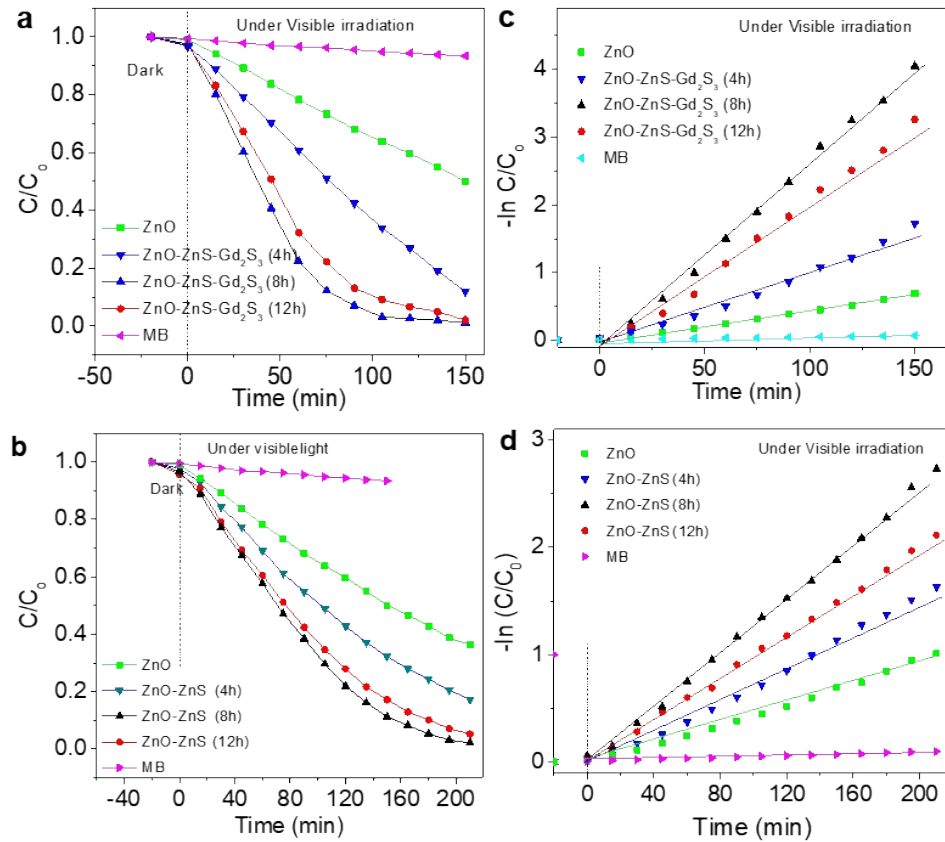


Fig. S9 (a-b) degradation rate (c-d) the plot of $\ln (C_0/C)$ with irradiation time of visible light, (C_0 is the initial concentration of MB after absorption; C is the concentration of MB after photoirradiation) for sulfidated ZnO NR arrays. (a, c) shell wall controlled ZnO-ZnS-Gd₂S₃ NR arrays and (b, d) shell wall controlled ZnO-ZnS NR arrays.

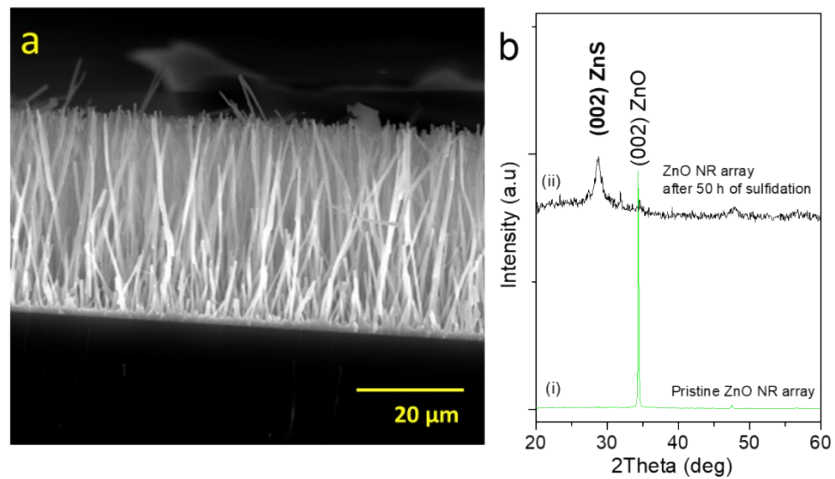


Fig. S10 (a) SEM and (b) XRD results of the 50 h sulfidated ZnO (ZnS NRs) NR arrays images.

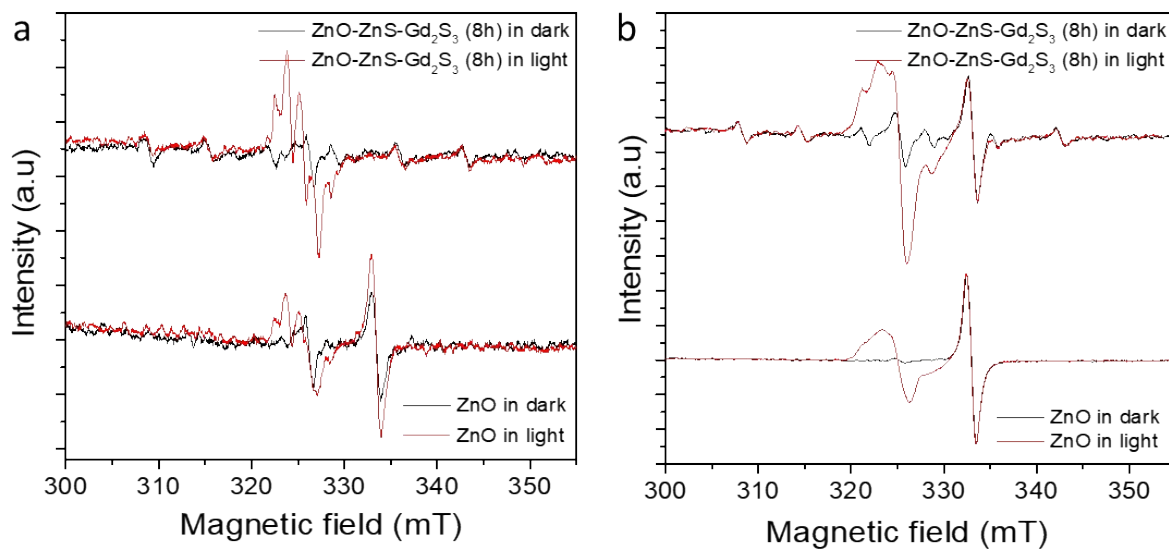


Fig. S11 ESR spectra of the radical adducts trapped by DMPO: (a) DMPO- O_2^- radical species detected from the sample dispersion in methanol, (b) DMPO-•OH radical species detected for the sample dispersion in water.

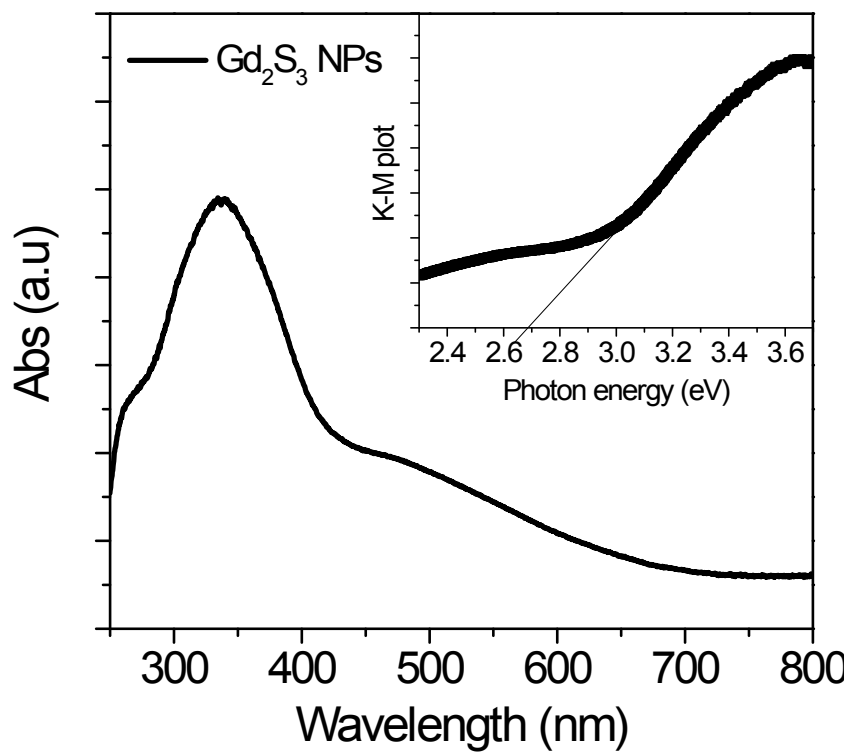


Fig. S12 UV DRS- absorbance spectra of the Gd_2S_3 nanoparticles and inset shows K-M plot of Gd_2S_3 nanoparticles.

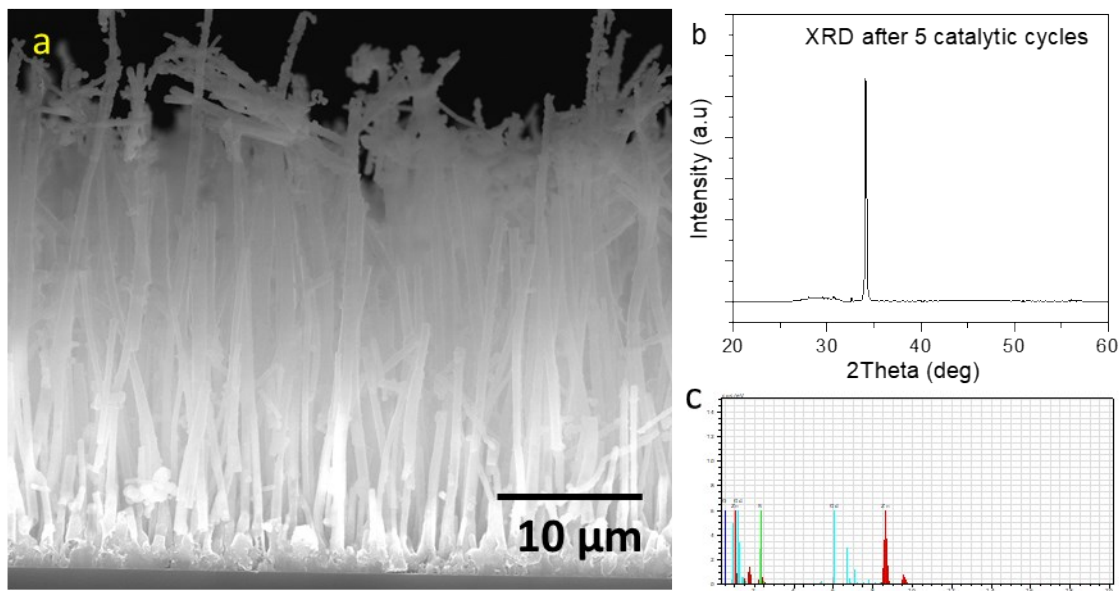


Fig. S13 (a) FESEM, (b) XRD and (c) EDX spectra of the ZnO-ZnS-Gd₂S₃ core-shell nanorod arrays after 5 reusable cycles.

Table S1. Chemical composition of the ZnO-ZnS-Gd₂S₃ NR array, which are calculated using ICP-MS results.

Sample	ICP-MS (wt %)
ZnO	Zn: 72.3
ZnO-ZnS	Zn: 54.5
ZnO-ZnS-Gd ₂ S ₃ (4h)	Zn: 61.8 Gd: 2.4
ZnO-ZnS-Gd ₂ S ₃ (8h)	Zn: 51.8 Gd: 7.3
ZnO-ZnS-Gd ₂ S ₃ (12h)	Zn: 48.4 Gd: 9.1